*Mol. Cryst. Liq. Cryst.*, Vol. 376, pp. 301-313

1058-725X/02 $12.00 + .00

# Molecular Nanomagnets

DAVID N. HENDRICKSON[a,*], GEORGE CHRISTOU[b,*], HIDEHIKO ISHIMOTO[c,*], JAE YOO[a], EUAN K. BRECHIN[b], AKIRA YAMAGUCHI[c], EVAN M. RUMBERGER[a], SHEILA M. J. AUBIN[a], ZIMMING SUN[a] and GUILLEM AROMI[b]

[a]*Department of Chemistry and Biochemistry-0358, University of California at San Diego, La Jolla, CA 92093-0358,*
[b]*Department of Chemistry, Indiana University, Bloomington, Indiana 47405 and*
[c]*Institute for Solid State Physics, The University of Tokyo, 7-22-1 Roppongi, Minatoku, Tokyo 106-8666, Japan*

**Abstract** Quantum mechanical tunneling of the direction of magnetization is discussed for several examples of single-molecule magnets (SMM's). Magnetization tunneling is described for two crystallographically different forms of $[Mn_{12}O_{12}(O_2CC_6H_4\text{-}p\text{-}Me)_{16}(H_2O)_4] \cdot$ solvate. The two $Mn_{12}$ complexes are isomers. The magnetization *versus* magnetic field hysteresis loops are quite different for the two isomeric $Mn_{12}$ complexes. One $Mn_{12}$ complex exhibits a magnetization hysteresis loop that is characteristic of considerably faster magnetization tunneling than in the other $Mn_{12}$ isomer. The unusual orientation of Jahn-Teller elongation axes in one isomer leads to greater rhombic zero-field splitting that is the origin of the faster magnetization tunneling. In addition to data for $Mn_{12}$ complexes, magnetization relaxation rate *versus* temperature responses of three mixed-valence $Mn_4$ complexes are also reported. In all three cases the Arrhenius plot of the logarithm of the magnetization relaxation rate *versus* the inverse absolute temperature shows a temperature-independent region as well as a temperature-dependent region. The temperature-independent relaxation rate is definitive evidence of magnetization tunneling in the lowest-energy zero-field component of the ground state.

**Keywords** Nanomagnet; Single-molecule magnet; Magnetization tunneling; Superparamagnet

## INTRODUCTION

Large metal cluster complexes with interesting magnetic properties characteristic of nanoscale magnetic particles, such as magnetization hysteresis loops and out-of-phase ac magnetic susceptibility signals, have been synthesized. In 1993 it was discovered that $[Mn_{12}O_{12}(O_2CCH_3)_{16}(H_2O)_4] \cdot 4H_2O \cdot 2CH_3CO_2H$ (**1**) (complex **1** or $Mn_{12}Ac$ for short), functions as a nanoscale magnet [1]. Such a molecule has been termed a single-molecule magnet (SMM). Since then, a few more families of complexes that function as SMM's have been obtained: 1) several other structurally related dodecanuclear manganese complexes, $[Mn_{12}O_{12}(O_2CR)_{16}(H_2O)_4]$ where R can be an aliphatic or aromatic group, and their corresponding singly reduced salts $[Mn_{12}O_{12}(O_2CCH_3)_{16}(H_2O)_4](PPh_4)$; [2-11] 2) several distorted $Mn_4$ cubane molecules with a $[Mn^{IV}Mn^{III}{}_3O_3X]^{6+}$ core [12], 3) a mixed-valent $[Mn_4(O_2CMe)_2(Hpdm)_6[ClO_4]_2$ [13], 4) tetranuclear vanadium (III) complexes with a butterfly structure [14]; and 5) a ferric complex $[Fe_8O_2(OH)_{12}(tacn)_6]^{8+}$, where tacn is triazacyclononane, which has been reported to display frequency-dependent out-of-phase peaks and magnetization hysteresis loops [15].

A SMM has a potential-energy barrier for reversal of its magnetic moment. In addition to thermal activation of each SMM over the barrier, the reversal of the direction of magnetization occurs via quantum mechanical tunneling through the barrier [16]. In this paper we will discuss some recent observations on SMM's that are manifestations of magnetization tunneling.

## ORIGIN OF SINGLE-MOLECULE MAGNETISM

Magnetization relaxation data on frozen solution or polymer-doped samples and the lack of any anomaly in heat capacity data collected in zero field confirm that the slow magnetization relaxation rates exhibited by these complexes are due to individual molecules rather than to long range ordering as is commonly observed in nanoscale magnetic domains [17]. The single-molecule magnetism behavior observed for the clusters shown in this paper originates from a combination of a large-spin ground state and a negative magnetoanisotropy. In the case of complex **1** high-field magnetization

and electron paramagnetic resonance (EPR) studies indicate that this complex has a high-spin ground state with S=10. The strong uniaxial magnetic anisotropy of the molecule originates from the single-ion zero field splitting experienced by the $Mn^{III}$ ions. This zero-field interaction splits the S=10 ground state into the different $m_s$=±10, ±9, ±8, ±7……..0 levels (see Figure 1). The negative magnetoanisotropy

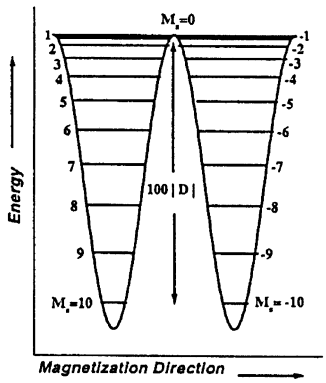


FIGURE 1. Plot of potential energy *vs.* the magnetization direction for a single molecule with an S=10 ground state split by axial zero-field splitting.

leads to a potential-energy barrier between the "spin up" (i.e., $m_s$=-10) and "spin down" (i.e., $m_s$=+10) orientations of the magnetic moment of an individual $Mn_{12}$ molecule. In order for a $Mn_{12}$ SMM to flip from "up" to "down", it has to either go over the barrier or it can tunnel through the barrier.

## RESULTS AND DISCUSSION

**Structures of complexes**. The occurrence of magnetization tunneling is discussed for two $Mn^{IV}_4Mn^{III}_8$, one $Mn^{IV}Mn^{III}_3$, and two $Mn^{III}_2Mn^{II}_2$ complexes. The complexes have the following formulas:

$$[Mn_{12}O_{12}(O_2CC_6H_4\text{-}p\text{-}Me)_{16}(H_2O)_4] \cdot (HO_2CC_6H_4\text{-}p\text{-}Me) \qquad \textbf{(2)}$$

$[Mn_{12}O_{12}(O_2CC_6H_4\text{-}p\text{-}Me)_{16}(H_2O)_4] \cdot 3H_2O$ **(3)**

$[Mn_4O_3Cl(O_2CMe)_3(dbm)_3]$ **(4)**

$[Mn_4(OAc)_2(pdmH)_6(H_2O)_4](ClO_4)_2$ **(5)**

$[Mn_4(hmp)_6Br_2(H_2O)_2]Br_2 \cdot 4H_2O$ **(6)**

The X-ray structures of complexes **4** [18] and **5** [19] have already been reported. Complex **4** has a distorted trigonal pyramidal arrangement of three $Mn^{III}$ ions with one $Mn^{IV}$ ion. This complex has a S = 9/2 ground state. In the case of **5** · 2MeCN · $Et_2O$, the cation consists of a planar $Mn_4$ rhombus that is mixed-valent $Mn^{III}_2Mn^{II}_2$. This solvated complex readily loses acetonitrile to give complex **5** that has been reported [19] to have a S = 8 ground state. Complex **6** is structurally similar to the tetranuclear complex **5** and has been found [20] to have a S = 9 ground state.

Complexes **2** and **3** have the well known $[Mn_{12}O_{12}(O_2CR)_{16}(H_2O)_4]$ structure. As a result of the different solvate molecules in the two crystals, complex **2** crystallizes in the *C*2/c space group, whereas complex **3** crystallizes in the *I*2/a space group [21]. Even though both of these complexes have the same ligands on the $Mn_{12}$ complexes, there are two significant differences in the molecular structures of the $Mn_{12}$ molecules in **2** and **3**. First, complexes **2** and **3** differ in the positioning of the four $H_2O$ ligands. Complexes **2** and **3** have one other very important difference in their structures. Each $Mn^{III}$ ion experiences a Jahn-Teller (JT) elongation. All of the JT elongation axes in the hydrate complex **3** are roughly parallel and perpendicular to the plane of the disc-like $Mn_{12}O_{12}$ core. For complex **2**, however, one JT axis is abnormally orientated. Complexes **2** and **3** have been determined [21] to have S = 10 ground states.

**Magnetization hysteresis loops for $Mn_{12}$ complexes.** Since complexes **2** and **3** have barriers for changing their magnetic moments from "spin up" to "spin down" (Figure 1), it is informative to examine the change in the magnetization of a sample as an external field is changed. For an oriented sample, steps can be seen at regular intervals of magnetic field in the magnetization hysteresis loop of a SMM. These steps result from a quantum mechanical tunneling of the

magnetization [22-25]. Oriented samples of complexes **2** and **3** were prepared by suspending a few small crystals of either complex in an eicosane wax cube.

Figure 2 shows the magnetization hysteresis data measured for complex **3**. Magnetization hysteresis loops are seen in the 1.72-2.50 K range. The coercive magnetic field and consequently the area enclosed within a hysteresis loop increase as the temperature is decreased.

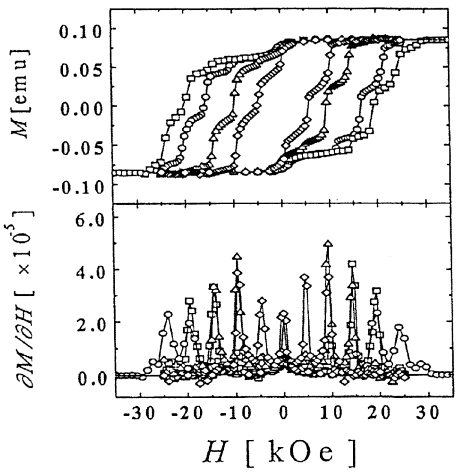


FIGURE 2. Plots of magnetization *versus* external magnetic field for $[Mn_{12}O_{12}(O_2CC_6H_4\text{-}p\text{-}Me)_{16}(H_2O)_4] \cdot 3H_2O$ (complex **3**) at five temperatures in the 1.72-2.50 K range. Five small crystals (1.2mg in total) were oriented in a frozen matrix so the magnetic field is parallel to the principle axis of magnetization.

Close examination of the magnetization hysteresis loops shown in Figure 2 for complex **3** shows that each hysteresis loop is not smooth, but steps are seen at regular intervals of the external field. These steps are due to tunneling of the magnetization. That is, a $Mn_{12}$ molecule in the "spin up" state can either be thermally activated over the barrier to

the "spin down" state or it reverses its direction of magnetization by tunneling through the barrier.

Magnetization hysteresis loops were also measured for the oriented eicosane cube of complex **2** at the temperatures of 1.72, 2.20, 2.00, 1.90 and 1.80 K (Figure 3). The hysteresis loops for complex **2** look quite different than those for complex **3**. When the external field is reduced from +2.5 T to zero, the magnetization falls off dramatically. The coercive fields are considerably less for complex **2** than for complex **3**. These two *p*-methylbenzoate $Mn_{12}$ complexes experience quite difference kinetic barriers for the reversal of magnetization. It must be emphasized that the sweep rate for all the loops was 25 Oe/s.

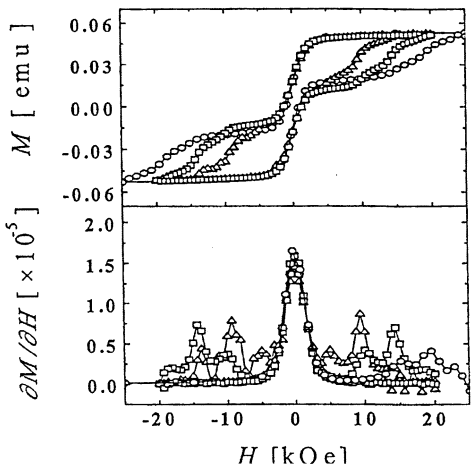


FIGURE 3. Plots of magnetization *versus* external magnetic field for $[Mn_{12}O_{12}(O_2CC_6H_4$-*p*-$Me)_{16}(H_2O)_4] \cdot (HO_2CC_6H_4$-*p*-Me) (complex **2**) at five temperatures in the 1.72-2.0 K range. Six small crystals (2.2 mg in total) were oriented in a frozen matrix so the magnetic field is parallel to the principle axis of magnetization.

From the hysteresis loop data it is clear that the *p*-methylbenzoate complex **2** has an appreciably greater rate of

magnetization relaxation than does isomeric complex **3**. This can be quantified by analyzing the frequency dependencies of the $\chi''_M$ signals for the two complexes reported previously [21]. Ac susceptibility data were collected at 8 different frequencies from 1.0 Hz to 1512 Hz for complex **3**. From the peaks in the $\chi''_M$ *vs.* temperature plots values of the magnetization relaxation time $\tau$ were determined at 8 temperatures. These data give a straight line Arrhenius plot of $\ln(1/\tau)$ *vs.* the inverse absolute temperature (1/T) for complex **3**. The data were least-squares fit to the Arrhenius eqn. (1) to give the parameters $\tau_0 = 7.7 \times 10^{-9}$ s and $U_{eff} = 64$ K.

$$\tau = \tau_0 \exp(U_{eff}/kT) \quad \textbf{(1)}$$

A similar analysis of the frequency dependence of the dominant low temperature $\chi''_M$ peak in the ac data for complex **2** gives $\tau_0 = 2.0 \times 10^{-10}$ s and $U_{eff} = 38$ K. The activation energy ($U_{eff}$) for reversal of the direction of the magnetization for complex **2** ($U_{eff} = 38$ K) is considerably less than that ($U_{eff} = 64$ K) for the isomeric complex **3**. The $Mn_{12}$acetate complex **1** has been reported [9] to have a $U_{eff}$ value of 62 K, very close to the value for complex **3**.

It is likely that the appreciably faster rate of magnetization tunneling observed for complex **2** compared to the isomeric complex **3** is due to the lower symmetry observed for complex **2**. This lowered symmetry would increase the rhombic zero-field splitting $[E(S_X^2 - S_y^2)]$ in the S = 10 ground state of complex **2** leading to an increase in the rate of magnetization tunneling. The importance of rhombicity in tunneling can be understood in the next section.

**Temperature-independent magnetization tunneling in complex 4.** In 1998 we reported [18] the presence of temperature-independent magnetization relaxation in the $Mn^{IV}Mn^{III}_3$ complex **4**. The complex $[Mn_4O_3Cl(O_2CMe)_3(dbm)_3]$ (**4**) where $dbm^-$ is the monoanion of dibenzoylmethane, has an S = 9/2 ground state [18]. Complex **4** shows magnetization hysteresis loops below 0.90 K, and steps are seen on each hysteresis loop. An Arrhenius plot of the magnetization relaxation data for complex **4** indicates a thermally activated region between 2.0 and 0.7 K and a temperature-independent region at temperatures below 0.70 K. A fit of the data in the temperature-dependent region gives $U_{eff} = 11.8$ K and $\tau_0 = 3.6 \times 10^{-7}$ s. With the D-

value obtained from HFEPR data for this S = 9/2 complex **4**, U can be calculated as 15.2 K (=10.6 $cm^{-1}$). It was concluded that the temperature-independent magnetization relaxation must correspond to magnetization tunneling between the lowest degenerate levels, the $M_s$ = 9/2 and –9/2 levels for the S = 9/2 complex **4**.

It is important to note that $Mn_4$ complex **4** shows tunneling in the lowest-energy level because this complex possesses relatively large transverse interactions. Due to its crystal site symmetry the $Mn_{12}$-acetate complex **1** has no rhombic zero-field splitting, and E = 0. Complex **4** probably shows tunneling in the lowest-energy level because each of these complexes is of lower symmetry and this gives a non-zero E value. The E term does not directly mix the $M_s$ = 9/2 and -9/2 states. The admixture will occur as a result of $E(\hat{S}_x^2 - \hat{S}_y^2)$ combined with other higher-order terms.

**Magnetization tunneling in the $Mn_4$ complexes 5 and 6.** Variable-field magnetization data have been fit [19] to determine that complex **5** has a S = 8 ground state with $D/k_B$ = -0.358 K. Ac magnetic susceptibility measurements have been carried out by cooling the sample with a $^3$He-$^4$He dilution refrigerator in the 0.4-3.5 K range. Eleven different AC frequencies were used (Figure 4 shows data taken at 5 different frequencies) in the 1.1-995 Hz range, which gave rates of magnetization reversal at 11 different temperatures. These relaxation data fit well to the Arrhenius equation to give an activation energy for magnetization reversal of $U_{eff}$ = 17.3 K with a preexponential factor of $\tau_0 = 2.54 \times 10^{-7}$ s. The thermodynamic barrier can be calculated to be U = 22.4 K. As with other SMM's, it is expected that $U > U_{eff}$, or the reversal of magnetization not only involves a thermal activation over the potential-energy barrier, but also quantum tunneling of the direction of magnetization.

The most definitive data showing that complex **5** does reverse its magnetization direction by quantum tunneling were obtained by means of magnetization decay experiments. In a DC magnetization decay experiment the sample is first cooled and maintained at low temperature, after which it is subjected to a very small magnetic field. At low temperatures, only a small field is needed to achieve magnetization saturation. The field is then suddenly removed and the magnetization is measured as a function of time. Over time the magnetization decays from some initial value at time zero, defined as

the time when the applied field becomes zero, to an equilibrium value. Plots of magnetization *versus* time were determined in the 0.030-0.860 K range for complex **5**. These magnetization decay data were fit to a

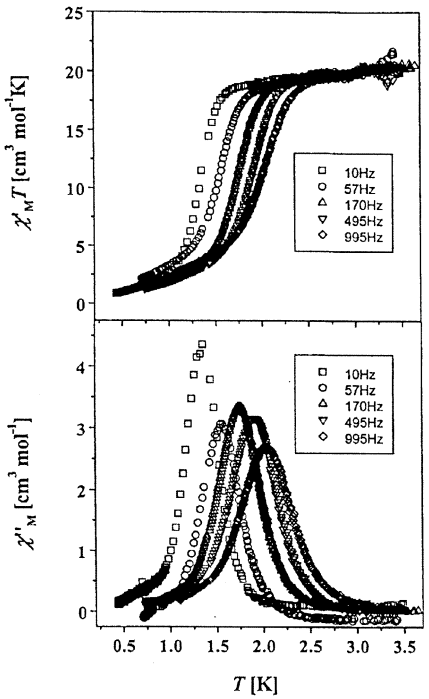


FIGURE 4. Plots of $\chi'_M$ (top) and $\chi''_M$ (bottom) *vs.* temperature for a polycrystalline sample of complex **5** in a 1.0 G AC field oscillating at the indicated frequencies, where $\chi'_M$ and $\chi''_M$ are the in-phase and out-of-phase susceptibilities, respectively.

stretched exponential function. This gave a set of relaxation times at temperatures in the 0.030-0.860 K range. It was found that at temperatures above ~0.5 K the magnetization relaxation time $\tau$ is temperature dependent.

The magnetization rate date obtained at higher temperatures for complex **5** with AC susceptibility measurements are combined with the DC magnetization decay rate data as an Arrhenius plot of $\ln(1/\tau)$ *versus* 1/T in Figure 5. This is indeed a very revealing plot, for it can be seen at temperatures above ~0.5 K the magnetization relaxation rate is temperature dependent with an activation energy of $U_{eff}$ = 17.3 K. However, at low temperatures below ~0.5 K, the relaxation rate is

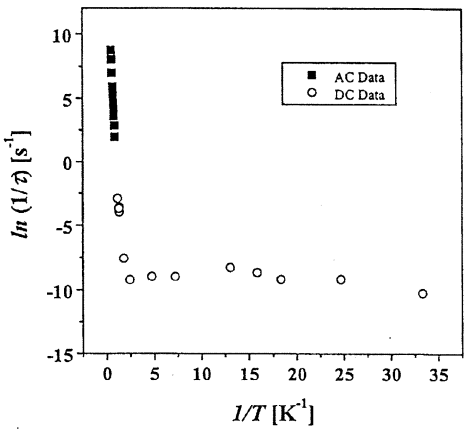


FIGURE 5. Plot of the natural logarithm of the relaxation rate ($1/\tau$) *vs.* the inverse temperature for complex **5**. The symbol ■ represents the data collected with the AC magnetic susceptibility technique, and the magnetization decay data are indicated by the symbol ○.

clearly temperature independent, indicating that the magnetization relaxation below this temperature is occurring purely by a quantum tunneling phenomenon. Complex **5** tunnels between the $m_s$ = -8 and $m_s$ = +8 levels at a rate of approximately $1 \times 10^{-4}$ $s^{-1}$.

Magnetization relaxation decay data were also collected for a sample of complex **6** in the 0.047-1.195 K range. This complex has a S = 9 ground state. The decay data were least-squares fit to give relaxation rates in the above temperatures range. These rates were

combined with those obtained at higher temperatures by means of the AC susceptibility technique as an Arrhenius plot. At the higher temperatures the relaxation rate is temperature dependent with an activation energy of 15.8 K. At the lower temperatures we again see a temperature-independent rate of relaxation. This surely attributable to ground state magnetization tunneling. The temperature-independent magnetization tunneling rate is $1 \times 10^{-3}$ $s^{-1}$ for complex **6**. Preliminary HFEPR data indicate that complex **6** experiences a larger rhombic zero-field splitting than does complex **5**. This would explain the faster rate of tunneling in complex **6**.

## ACKNOWLEDGMENTS

D.N.H. and G.C. thank the National Science Foundation for support of this research.

## REFERENCES

[1] (a) R. Sessoli, D. Gatteschi, A. Caneschi, M. Novak, Nature **365,** 149(1993). (b) H. J. Eppley, H. –L. Tsai, N. de Vries, K. Folting, G. Christou, D. N. Hendrickson, J. Am. Chem. Soc. **117,** 301(1995).

[2] T. Lis, Acta Cryst. B36, 2042(1980)

[3] P.D. Boyd, Q. Li, J. B. Vincent, K. Folting, H. –R. Chang, W. E. Streib, J. C. Huffman, G. Christou, D. N. Hendrickson, J. Am. Chem. Soc. **110**, 8537(1998).

[4] A. Caneschi, D. Gatteschi, R. Sessoli, A. L. Barra, L. C. Brunel, M. Guillot, J. Am. Chem. Soc. **113**, 5873(1991).

[5] (a) D. Ruiz, Z. Sun, B. Albela, K. Folting, J. Ribas, G. Christou, D. N. Hendrickson, Angew. Chemie. In. Ed. Engl. **37**, 300(1988). (b) D. Ruiz, Z. Sun, S. M. J. Aubin, E. Rumberger, C. Incarvito, K. Folting, A. L. Rheingold, G. Christou, D. N. Hendrickson, Mol. Cryst. And Liq. Cryst. **335**, 371(1999). (c) S. M. J. Aubin, D. Ruiz, E. Rumberger, Z. Sun, B. Albela, M. Wemple, N. R. Dilley, J. Ribas, M. B. Maple, G. Christou, D. N. Hendrickson, Mol. Cryst. And Liq. Cryst. **335**, 371(1999).

[6] R. Sessoli, H. –L. Tsai, A. R. Schake, S. Wang, J. B. Vincent, K. Folting, D. Gatteschi, G. Christou, D. N. Hendrickson, J. Am. Chem. Soc. **115**, 1804(1193),

[7] S.M.J. Aubin, Z. Sun, I. A. Guzei, A. L. Rheingold, G. Christou, D. N. Hendrickson, Chem Comm., 2239(1997).

[8] Z. Sun. D. Ruiz, E. Rumberger, C. Incarvito, A. L. Rheingold, G. Christou, D. N. Hendrickson, Inorg. Chem. **37**, 4758(1998)

[9] H. –L. Tsai, H. J. Eppley, N. Devries, K. Folting, D. N. Hendrickson, G. Christou, Chem Comm. **15.** 1745(1994)

[10] S. M. J. Aubin, S. Spagna, H. J. Eppley, R. E. Sager, G. Christou, D. N. Hendrickson, Chem. Comm. **7**, 803(1998). (b) S. M. J. Aubin, Z. Sun, L. Pardi, J. Krzystek, K. Folting, L. C. Brunel, A. L. Rheingold, G. Christou, D. N. Hendrickson, Inorg. Chem., *in press*.

[11] K. Takeda, K. Awaga, T. Inabe, Phys. Rev. B. **57**, 110621(1998).

[12] (a) S. M. J. Aubin, N. R. Dilley, M. W. Wemple, M. B. Maple, G. Christou, D. N. Hendrickson, J. Am. Chem. Soc. **120**, 869(1998). (b) S. M. J. Aubin, N. R. Dilley, L. Pardi, J. Krzystek, M. W. Wemple, L. C. Brunel, M. B. Maple, G. Christou, D. N. Hendrickson, J. Am. Chem. Soc. **120**, 4991(1998).

[13] E. K. Brechin, J. Yoo, M. Nakano, J. C. Huffman, D. N. Hendrickson, G. Christou, Chem Comm. **9**, 783(1999),

[14] (a) Z. Sun, C. M. Grant, S. L. Castro, D. N. Hendrickson, G. Christou, Chem. Comm. **6**, 721(1998). (b) S. L. Castro, Z. Sun, C. M. Grant, J. C. Bollinger, D. N. Hendrickson, G. Christou, J. Am. Chem. Soc. **120**, 2365(1998).

[15] (a) A. –L. Barra, P. Debrunner, D. Gatteschi, C. E. Schulz, R. Sessoli, Europhys. Lett. **35**, 133(1996). (b) C. Sangregorio, T. Ohm, C. Paulsen, R. Sessoli, D. Gatteschi, Phys. Rev. Lett. **78**, 4645(1997).

[16] G. Christou, D. Gatteschi, D. N. Hendrickson, R. Sessoli, M.R.S. Bulletin, **25**, 66(2000).

[17] M. A. Novak, R. Sessoli, A. Caneschi, D. Gatteschi, J. Magn. Magn. Mater. **146**, 211(1995).

[18] S. M. J. Aubin, N. R. Dilley, L. Pardi, J. Krzystek, M. W. Wemple, L. –C. Brunel, M. B. Maple, G. Christou, D. N. Hendrickson, J. Am. Chem. Soc. **120**, 4997(1998).

[19] J. Yoo, E. K. Brechin, A. Yamaguchi, M. Nakano, J. C. Huffman, A. L. Maniero, L. –C. Brunel, K. Awaga, H. Ishimoto, G. Christou, D. N. Hendrickson, Inorg. Chem. **39**, 3615(2000).

[20] J. Yoo, A. Yamaguchi, M. Nakano, J. Krzystek, W. E. Streib, L. –C. Brunel, H. Ishimoto, G. Christou, D. N. Hendrickson, submitted for publication.
[21] S. M. J. Aubin, Z. Sun. H. J. Eppley, E. M. Rumberger, I. A. Guzei, K. Folting, P. K. Gantzel, A. L. Rheingold, G. Christou, D. N. Hendrickson, Inorg. Chem. **40**, 2127(2001).
[22] J. R. Friedman, M. P. Sarachik, J. Tejada, J. Maciejewski, R. Ziolo, J. Appl. Phys. **79**, 6031(1996).
[23] J. R. Friedman, M. P. Sarachik, J. Tejada, R. Ziolo, Phys. Rev. Lett. **76**, 3830(1996).
[24] L. Thomas, F. Lionti, F. R. Ballou, D. Gatteschi, R. Sessoli, B. Barbara, Nature, **383**, 145(1996).
[25] J. Tejada, R. Ziolo, X. X. Zhang, Chem. Mater, **8**, 1784(1996).